Observation of Spontaneous Toroidal Rotation Inversion in Ohmically Heated Tokamak Plasmas

A. Bortolon, B. P. Duval, A. Pochelon, and A. Scarabosio

Ecole Polytechnique Fédérale de Lausanne (EPFL)–Centre de Recherches en Physique des Plasmas (CRPP), Association Euratom-Confédération Suisse. CH-1015 Lausanne, Switzerland

(Received 16 August 2006; published 8 December 2006)

Bulk plasma toroidal rotation is observed to invert spontaneously from counter to cocurrent direction in TCV (Tokamak à Configuration Variable) Ohmically heated discharges, in low confinement mode, without momentum input. The inversion occurs in high current discharges, when the plasma electron density exceeds a well-defined threshold. The transition between the two rotational regimes has been studied by means of density ramps. The results provide evidence of a change of the balance of nondiffusive momentum fluxes in the core of a plasma without an external drive.

DOI: 10.1103/PhysRevLett.97.235003 PACS numbers: 52.55.Fa, 52.25.Fi, 52.30.−q

Considerable effort has been expended in the experimental study of momentum transport in magnetically confined Tokamak plasmas, since the rotation state of the plasma is found to have a direct impact on the global energy and/or particle confinement. Well known examples are the stabilization of resistive wall modes in rotating plasmas [1,2] and the enhanced confinement regimes, where the radial shear of plasma flows can lead to turbulence suppression, observed when the plasma configuration transits from low (L mode) to high confinement regime (H mode), or at the formation of internal transport barriers (ITBs) [3–5]. In many present-day fusion devices, plasma momentum is supplied externally by the tangential injection of heating neutral beams. The presence of a substantial intrinsic toroidal rotation has also been observed in plasmas with no externally applied torque [6], which could determine a possibility of sustaining the rotation profile in next step devices, where the toroidal momentum driven by auxiliary heating systems may not dominate that generated by the plasma itself [7]. To date, the physical mechanisms generating the angular momentum, within the plasma, remain an open issue with, in particular, a strong debate as to whether the momentum source is mostly localized in the plasma core or at the edge. For the relatively simple Ohmically heated L mode configurations, previous studies indicate that particle flows outside the last closed magnetic surface can drive a net contribution to core plasma rotation [8], whereas recent measurements of edge rotation profiles, that approach zero values at the plasma edge [9], suggest a negligible momentum transfer from the edge.

This Letter reports toroidal rotation measurements of tokamak plasmas in limited L mode configuration, with negligible external momentum input, supporting the presence of nondiffusive momentum fluxes located in the core of the plasma (internal momentum sources). In this configuration, we first observed a spontaneous transition of plasma rotation from countercurrent to cocurrent direction when the plasma density exceeded a well defined threshold (Fig. 1). Transition between these two regimes was studied by ramping the plasma density across this threshold, directly investigating the internal momentum balance. The experiments were conducted in TCV (Tokamak à Configuration Variable), a medium sized tokamak ($R = 0.88$ m, $a = 0.25$ m, $B_t = 1.45$ T, $I_p < 1$ MA), with an elongated ($\kappa = 3$) vacuum vessel and a flexible control system, that can generate a wide variety of plasma shapes [10]. Momentum transport is studied using temporally resolved velocity profiles provided by the TCV charge exchange recombination spectroscopy (CXRS) diagnostic [11]. Toroidal velocity is measured from the Doppler shift of the 529.1 nm charge exchange emission from the interaction of carbon impurity ions with the TCV diagnostic neutral beam (DNBI) [12]. In the used configuration, 8 local measurements along the plasma minor radius are acquired with a sample frequency of 10–20 Hz with an

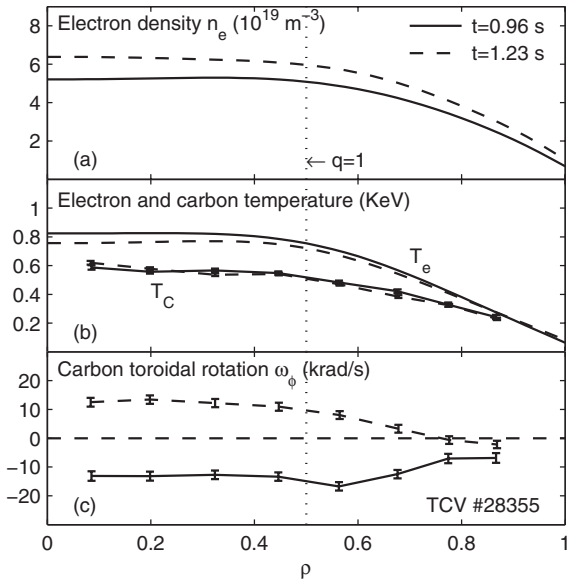

FIG. 1. Electronic density (a), electron and carbon temperatures (b), and angular velocity (c) profiles, below (solid) and above (dashed) the electron density threshold.

integration time of 15–30 ms. It is to be stressed that the rotation induced by the DNBI beam (estimated ≈ 1 km/s) is small compared to values typically measured, due to a combination of quasi orthogonal injection angle (11°) and modest deposited power (20 kW). No other external momentum input is present in TCV.

Figure 1 shows the radial profiles of density (n_e), temperature (T_e) and toroidal rotation (ω_ϕ), measured in a deuterium discharge, with plasma current $I_p = 340$ kA, for two central density values. The radial coordinate corresponds to the square root of normalized poloidal flux, $\rho = \sqrt{\psi/\psi_a}$. For $n_{e0} \sim 5.2 \times 10^{19}$ m^{-3} (solid curves) the plasma rotates toroidally in the counter direction with respect to the plasma current (electron diamagnetic drift direction, negative values), as often measured in other tokamaks in this regime [8]. The rotation profile (c) is flat, or slightly hollow, inside the sawtooth inversion radius ($q = 1$ at $\rho \approx 0.5$), with central values of $\omega_\phi \sim -10$ krad/s, corresponding to $v_\phi = \omega_\phi R = -11.4$ km/s. The toroidal rotation amplitude decreases away from the center approaching zero in the plasma edge region ($\rho > 0.9$). These general features are similar for a large range of TCV plasmas with plasma currents ranging from 100 to 350 kA and central electron densities up to 6×10^{19} m^{-3} [9]. In this countercurrent rotation regime, the maximum absolute rotation depends approximately linearly on the ion temperature, as summarized by a scaling law proposed in [9], $v_{\phi,\max}[\text{km/s}] = -12.5 T_{C0}/I_p[\text{eV/kA}]$ where $v_{\phi,\max}$ is the maximum toroidal velocity along the profile, T_{C0} the central ion (carbon) temperature.

This behavior changes when high density ($n_{e0} > 6 \times 10^{19}$ m^{-3}) and high current ($I_p > 290$ kA) are simultaneously attained. Here a different regime occurs, with the central toroidal rotation now directed with the plasma current (ion diamagnetic drift direction). The dashed curve in Fig. 1(c) shows the angular velocity profile measured, after increasing the density to $n_{e0} \sim 6.4 \times 10^{19}$ m^{-3} within the same discharge. The plasma core now rotates in the ion diamagnetic direction up to $\rho \sim 0.7$ with a flat or slightly centrally peaked profile, and a central velocity of $\omega_\phi \sim 12$ krad/s. The outermost CXRS measurements indicate that the rotation in the external region is still countercurrent. The two rotational states occur for similar temperature and density profiles [Figs. 1(a) and 1(b)], that are both flat inside the sawtooth inversion radius. In the central region n_e has increased from 5.2 to 6.4×10^{19} m^{-3} whereas T_e has only slightly decreased. In particular the T_i profile is constant across the transition, to within the measurement uncertainty. Time traces of the main plasma parameters are shown in Fig. 2 for the same discharge. The current flat top starts at 0.4 s; from $t = 0.5$ s to $t = 1.5$ s the central electron density is ramped up from 3 to 7×10^{19} m^{-3}. During the ramp, T_e decreases from 1 to 0.8 keV, with T_C increasing from 450 to 600 eV due to the increased collisional heat exchange between electrons and carbon ions. At the start of the density ramp ($t = 0.5$ s), the central toroidal rotation is approximately zero. A countercurrent acceleration follows, as T_C increases. This behavior ceases at $t = 1.1$ s, when the plasma core velocity changes rapidly from -14 to $+10$ krad/s, within 100 ms, to flow in the cocurrent direction. After this transition, the toroidal velocity and T_C are maintained until the discharge termination, although the density ramp continues. The time scale for the transition ($\tau_{\text{inv}} \approx 0.1$ s) is considerably faster than that of any global variation in the main plasma parameters, as seen in Fig. 2. Nevertheless, in this 100 ms time window, the total angular momentum of the plasma column carried by the carbon plasma component (n_C profile measured by CXSR) evolves from negative value of -10×10^{-5} to positive value of 1×10^{-5} J s: a net increment of 11×10^{-5} J s [Fig. 2(d)].

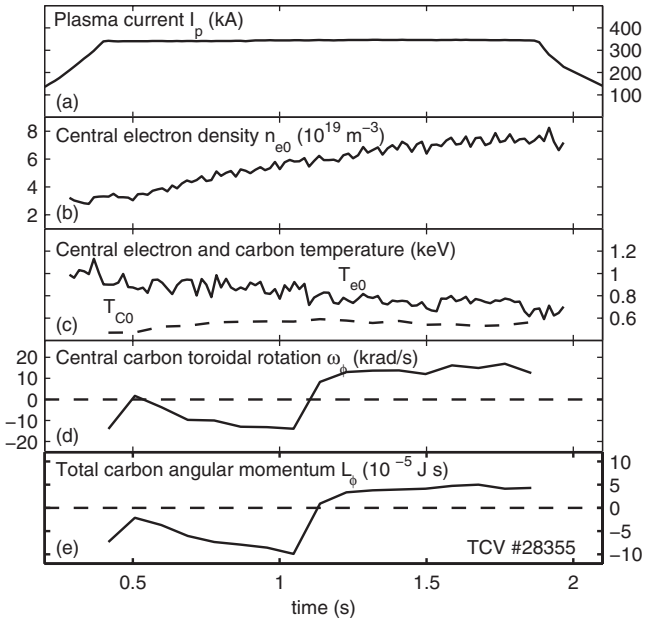

FIG. 2. Characteristic time traces of discharge parameters, from top to bottom: plasma current, central electron density, central electron and carbon temperature, central carbon toroidal rotation, and total angular momentum. Positive values indicate flows in the ion diamagnetic direction (cocurrent).

The rotation inversion was reproduced for a number of similar discharges: delaying (or advancing) the density ramp resulted in a later (earlier) inversion, at a density threshold of $n_{e0} \sim 6 \times 10^{19}$ m^{-3}, at $I_p = 340$ kA. In discharges with higher I_p the inversion occurs at slightly lower density ($n_{e0,\text{thr}} \approx 5.8 \times 10^{19}$ m^{-3} for $I_p = 380$ kA). No inversion was observed in discharges for $I_p < 290$ kA. The rapid change in the rotational state of the plasma was confirmed by soft x-ray (SXR) and magnetic measurements, in discharges where sawtooth precursor oscillations were present. Figure 3 shows the spectrogram of the SXR emissivity at the radial position of the mode ($\rho = 0.6$), during a density ramp up discharge at $I_p = 320$ kA. Precursor oscillations, whose frequency provides an estimate of plasma rotation, are visible as narrow ver-

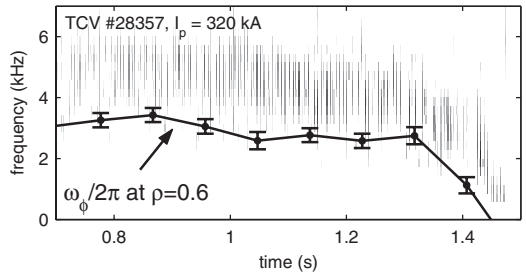

FIG. 3. Spectrogram of soft x-ray emissivity and toroidal rotation frequency (solid curve) at the position of sawtooth precursor mode.

tical bands before each sawtooth crash. The frequency corresponding to carbon rotation measured by the CXRS ($\omega_\phi/2\pi$) is also shown for comparison. The time evolution of the precursor frequency agrees well with the CXRS measurements (the discrepancy in the absolute values is often observed in TCV for small MHD instabilities and decreases for larger MHD modes [13]). In particular, for $t > 1.3$ s the precursor frequency drops from 5 kHz to approximately zero, simultaneously with the rotation inversion, providing an independent measurement of the deceleration of the plasma column. Later in the discharge, the precursor is no longer detectable.

The transition was found to be reversible. Figure 4(a) shows the time evolution of central electron density and carbon toroidal rotation, for a discharge where the plasma density was first ramped over the threshold and then reduced by cutting the gas feed, on a time scale mainly determined by the wall recycling. At $t = 0.9$ s, the transition density threshold is reached ($n_{e0} \approx 6 \times 10^{19}$ m^{-3}) and the plasma rotation inverts. During the subsequent n_e decrease, ω_ϕ decreases slowly (as does T_i, not shown) until the rotation reverses back to the countercurrent direction at $t = 1.55$ s, at a lower density of $n_{e0} = 4.4 \times 10^{19}$ m^{-3}. The locus of $\omega_{\phi 0}$ against n_{e0} (Fig. 4) shows that the central rotation after the back inversion recovers its preinversion values, for the same central density. The evolution of n_{e0} and ω_ϕ indicates a hysteresis on the electron density, suggesting a more complex dependence on plasma parameters. A similar hysteresis was observed in discharges with constant $n_{e0} > 6.0 \times 10^{19}$ m^{-3} by ramping $I_p > 290$ kA and then decreasing the I_p, with the back inversion consistently occurring at lower plasma current. Beyond the n_e threshold, the plasma rotation profiles are governed by a changed balance between components of angular momentum. Figure 5(a) shows the rotation profile evolution for a discharge where a slower transition ($\tau_{\text{inv}} \approx 200$ ms) was observed with an increased CXRS sampling rate (20 Hz). Profiles corresponding to measurements before, during and after the inversion are shown. The change of the rotation profile first appears in the central part of the plasma column up to $\rho \approx 0.7$, while the edge rotation is unchanged, to measurement uncertainties. The next profile corresponds to the plasma core rotation crossing $\omega_\phi = 0$ krad/s: the central plasma region, $\rho < 0.6$, appears to accelerate rigidly in the cocurrent direction. During inversion, the outermost CXRS chord, $\rho = 0.85$, shows a transitory increased negative velocity of ~ -7 krad/s. This was studied by high spatial edge resolution measurements in discharges where the plasma axis was vertically displaced, such that the CXRS diagnostic chords observed the plasma edge. Figure 5(b) shows the edge toroidal rotation profiles across an inversion for a discharge with $I_p = 340$ kA: rotation inversion takes place at $t = 1.15$ s and affects the plasma up to $\rho \approx 0.8$; for more external radii, the rotation for the standard (counter) and inverted (cocurrent) regimes is always ≈ 0 krad/s.

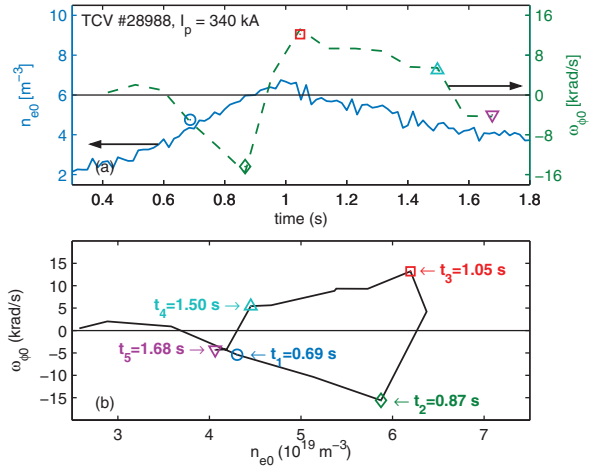

FIG. 4 (color). (a) Temporal evolution of central density (solid) and central toroidal rotation (dashed) for a discharge featuring a density ramp up followed by a density ramp down. The locus of n_{e0} and $\omega_{\phi 0}$ (b) indicates hysteresis on the electronic density parameter.

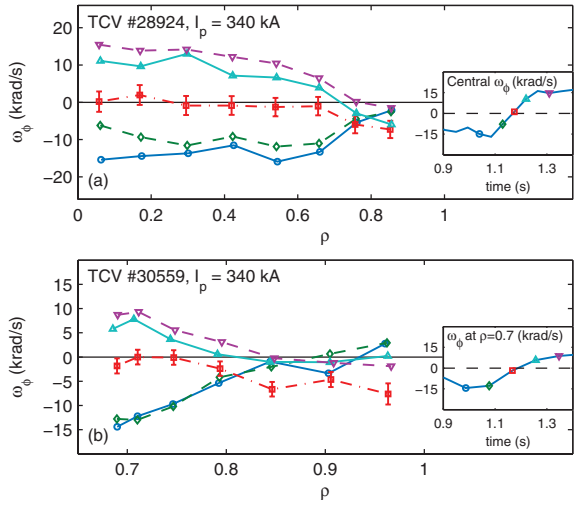

FIG. 5 (color). Temporal evolution of the core (a) and edge (b) angular velocity profiles across a toroidal rotation inversion. The change of rotation affects the central part of the plasma. After the inversion, ω_ϕ for $\rho > 0.85$ recovers its former values.

The plasma core deceleration >10 krad/s was accompanied by an increase (in the counter direction) of the plasma edge rotation of ~5 krad/s. These observations are not consistent with a diffusive flux of angular momentum from the edge region due to plasma viscosity, implying that the plasma has suffered a change in the balance of internally generated sources (nondiffusive fluxes) of toroidal momentum. The transient edge acceleration in opposite direction may be ascribed to total momentum conservation, which is not observed on time scales longer than ~50 ms, where the excess momentum is thought to be dissipated on the vessel wall within the resolution of our CXRS diagnostic.

An initial qualitative interpretation may be attempted from these results. MHD activity appears to play a minor role in the process: even if MHD modes can strongly influence the rotation profile [14], in these discharges, except for sawteeth, very little activity was observed. In addition, no rapid change in the sawtooth period (T_{st} ~ 6–8 ms), amplitude or inversion radius is observed across the transition. A possible link between the rotation inversion and the particle/energy transport comes from the force balance equation for the carbon impurity:

$$E_r = \frac{\nabla p_C}{n_C Z_C e} - (v_\phi B_\theta - v_\theta B_\phi)$$

where E_r is the radial electric field, $\nabla p_C/Z_C e$ the diamagnetic term, with $p_C = n_C T_C$ the carbon pressure, B is the magnetic field, and v the plasma velocity (ϕ and θ indicate the toroidal and poloidal vectorial components). Across the transition the diamagnetic term varies slowly (Fig. 1). If this holds also for v_θ (as predicted by neoclassical theory and observed in preliminary poloidal CXRS measurements), the inversion of toroidal rotation directly reflects a change in the E_r profile. In tokamak plasmas the radial electric field is often determined by the transport regime, which may change during the performed density ramps. For example with increasing density, the ion neoclassical transport rates (due to Coulomb collisions) become increasingly important and possibly comparable to the anomalous electron transport rates, as reported in [15]. At the same time, the type of turbulence responsible for anomalous transport may also depend on plasma parameters that vary during the density ramp: T_e, T_C, n_e, etc. Experiments with up to 500 kW of centrally deposited second harmonic electron cyclotron heating were performed to test the inversion process dependence on T_e profile, without affecting T_C profile. The density threshold was seen to increase in presence of higher core T_e (T_{e0} = 1 keV, $n_{e0,\mathrm{thr}} = 6.5 \times 10^{19}$ m^{-3} for I_p = 340 kA), indicating that the parameter driving the transition must, at least, contain terms depending on T_e and n_e. Collisionality has been considered, as it strongly influences the particle and energy transport, especially close to the transition from trapped electron mode to ion temperature gradient mode dominated turbulence [16–18]. However, at the present stage, this hypothesis lacks clear experimental vindication.

In conclusion, a change of rotation regime has been observed in relatively simple Ohmically heated L mode configuration TCV tokamak plasmas. The intrinsic toroidal rotation is seen to invert direction spontaneously, from cocurrent to countercurrent direction, when the plasma density exceeds a well defined threshold. The phenomenon is highly reproducible with a database of many discharges assembled in which the rotation inversion was obtained by ramping the plasma density over the threshold. The transition from cocurrent to countercurrent rotation was faster than any variation of major plasma profiles and mainly affected the plasma core. This experimental evidence proves that there is a rapid change in the balance of nondiffusive fluxes of toroidal momentum in the core of the plasma. The reported phenomenology extends the experimental domain of bulk rotation in the low confinement regime and defines a unique test for momentum transport models of tokamak plasmas.

The authors would like to acknowledge A. Karpushov and Y. Andrebe for their work with the DNBI and CXRS diagnostics, and O. Sauter for very helpful discussions. This work was supported in part by the Swiss National Science Foundation.

[1] E. J. Strait *et al.*, Phys. Rev. Lett. **74**, 2483 (1995).
[2] L.-J. Zheng, M. Kotschenreuther, and M. S. Chu, Phys. Rev. Lett. **95**, 255003 (2005).
[3] K. H. Burrel, Phys. Plasmas **4**, 1499 (1997).
[4] R. J. Groebner, K. H. Burrell, and R. P. Seraydarian, Phys. Rev. Lett. **64**, 3015 (1990).
[5] K. Crombé *et al.*, Phys. Rev. Lett. **95**, 155003 (2005).
[6] I. H. Hutchinson, J. E. Rice, R. S. Granetz, and J. A. Snipes, Phys. Rev. Lett. **84**, 3330 (2000).
[7] Special issue on ITER Physics Basis [Nucl. Fusion **39**, 2175 (1999)].
[8] J. E. Rice *et al.*, Nucl. Fusion **45**, 251 (2005).
[9] A. Scarabosio *et al.*, Plasma Phys. Controlled Fusion **48**, 663 (2006).
[10] F. Hofmann *et al.*, Plasma Phys. Controlled Fusion **36**, B277 (1994).
[11] A. Bortolon *et al.*, in *Proceedings of the 32nd EPS Conference on Plasma Physics, Tarragona, 2005* [Europhys. Conf. Abstr. **29C**, P4.098 (2005)].
[12] A. N. Karpushov *et al.*, Fusion Eng. Des. **66–68**, 899 (2003).
[13] A. Scarabosio *et al.*, in *Proceedings of the 32nd EPS Conference on Plasma Physics, Rome, 2006* [Europhys. Conf. Abstr. **30I**, P1.151 (2006)].
[14] A. Scarabosio *et al.*, in Ref. [11] [Europhys. Conf. Abstr. **29C**, P1.049 (2005)].
[15] M. Murakami *et al.*, Phys. Rev. Lett. **42**, 655 (1979).
[16] Y. Camenen *et al.*, Plasma Phys. Controlled Fusion **47**, 1971 (2005).
[17] C. Angioni *et al.*, Phys. Rev. Lett. **90**, 205003 (2003).
[18] F. Ryter *et al.*, Phys. Rev. Lett. **95**, 085001 (2005).